Overview of the Numerics of the ECMWF Atmospheric Forecast Model

Mariano Hortal

ECMWF
Shinfield Park, Reading, UK

1. Introduction

The dynamical part of the ECMWF atmospheric forecast model has been developed over a number of years jointly between ECMWF and Météo-France. Many people have contributed, both from the scientific and from the technical points of view, to the continual improvements of both its accuracy and its efficiency.

A basic requirement of the model code from its inception has been its portability, having to run efficiently in both vector and scalar computers and in single processors or massively parallel architectures. This gives ECMWF freedom in the process of choosing a new supercomputer when the need arises.

The main characteristics of the present operational atmospheric forecast model are:

- The vertical coordinate is a hybrid pressure-based coordinate.
- It uses the hydrostatic and the shallow-atmosphere approximations in the governing equations.
- The time integration is a two-time-level semi-Lagrangian semi-implicit scheme.
- The horizontal representation is spectral using spherical harmonics as basis functions.
- The vertical integrals are performed with an operator developed using the finite-element (pseudo-spectral) technique.
- In both the horizontal and the vertical, the transform method is used to compute non-linear terms. The corresponding grid in physical space is non-staggered.
- A fourth order horizontal diffusion is applied to reduce the amplitude of the shortest scales of motion.

These characteristics of the ECMWF forecast model are described in more detail in sections 2 to 10 below.

2. The vertical coordinate

The vertical coordinate η is a pressure-based coordinate very similar to the "hybrid" coordinate described by Simmons and Burridge (1981). It is chosen to have the value 0 at the top of the atmosphere (p=0) and the value 1 at the surface of the model.

The coordinate is defined as a monotonic function of pressure specified by means of two arbitrary functions $A(\eta)$ and $B(\eta)$ so that:

$$\frac{\partial p}{\partial \eta} = \frac{dA(\eta)}{d\eta} + \frac{dB(\eta)}{d\eta} p_s \qquad (1)$$

where p is the pressure and p_s the surface pressure. $A(\eta)$ is zero near the surface of the model, and therefore the η coordinate is a σ coordinate there, which follows the contour of the orography. The shape of function $B(\eta)$ is chosen to vary smoothly from 1 at the surface to zero in the upper atmosphere. In the region of the atmosphere where $B(\eta)=0$, η is a pure pressure coordinate.

In order to have the value of η equal to 1 at the surface of the model, or expressed differently, that the pressure at the surface, as found by integration of (1) from the top of the atmosphere (η=0) to the surface (η=1) is $p_{s,,}$ the two conditions

$$\int_0^1 \frac{dA}{d\eta} d\eta = 0\,; \quad \int_0^1 \frac{dB}{d\eta} d\eta = 1 \tag{2}$$

should be accurately fulfilled with the numerical integration scheme used in the vertical in the model.

The number of levels in the operational model is 60, with the top level at 0.1 hPa. A new distribution is being tested in which the resolution is increased everywhere but mostly near the tropopause. The total number of levels in the new distribution is 91, with the topmost level at 0.01 hPa.

3. Governing equations of the forecast model

We use the hydrostatic primitive equation set, with the momentum equations written in vector form to avoid pole problems. The equations are written in Lagrangian form, i.e. using total time derivatives, consistent with the semi-Lagrangian treatment of the advection (see later). The evolution equations, using the hybrid vertical coordinate η described in Section 2, are (see Ritchie et al 1995)

Momentum equation:

$$\frac{d\vec{V}_h}{dt} = -f\vec{k}\times\vec{V}_h - \nabla_h\phi - R_d T_v \nabla_h \ln p + P_V + K_V \tag{3}$$

Thermodynamic equation:

$$\frac{dT}{dt} = \frac{\kappa T_v \omega}{(1+(\delta-1)q)\,p} + P_T + K_T \tag{4}$$

Hydrostatic equation:

$$\phi = \phi_s - \int_1^{\eta} R_d T_v \frac{\partial}{\partial \eta}(\ln p) d\eta \tag{5}$$

Continuity equation:

$$\frac{\partial}{\partial t}\left(\frac{\partial p}{\partial \eta}\right) + \nabla_h \cdot \left(\vec{V}_h \frac{\partial p}{\partial \eta}\right) + \frac{\partial}{\partial \eta}\left(\dot{\eta}\frac{\partial p}{\partial \eta}\right) = 0 \tag{6}$$

Humidity equation:

$$\frac{dq}{dt} = P_q \tag{7}$$

Ozone equation:

$$\frac{dr_{o_3}}{dt} = P_{o_3} \tag{8}$$

Here $\vec{V}_h$ is the horizontal wind vector, T_v the virtual temperature, ∇_h the "horizontal" gradient operator (along surfaces of constant η, which are the model levels), ω the pressure vertical velocity ($\equiv dp/dt$), $\kappa \equiv R_d / c_{pd}$, $\delta \equiv c_{pv} / c_{pd}$, ϕ the geopotential, P_x the contributions from the physical parameterizations and K_x the contribution from the horizontal diffusion.

The term $\nabla_h\phi - R_d T_v \nabla_h \ln p$ is called the pressure-gradient term.

The continuity equation is integrated in the vertical to give:

a) the surface pressure tendency:

$$\frac{d}{dt}(\ln p_s) = \int_0^1 (\frac{dB}{d\eta}\frac{\partial}{\partial t}(\ln p_s) + \frac{dB}{d\eta}\vec{V}_h \cdot \nabla \ln p_s) d\eta \tag{9}$$

where

$$\frac{\partial}{\partial t}(\ln p_s) = -\frac{1}{p_s}\int_0^1 \nabla \cdot (\vec{V}_h \frac{\partial p}{\partial \eta}) d\eta$$

b) the pressure vertical velocity:

$$\omega = -\int_0^\eta \nabla \cdot (\vec{V}_h \frac{\partial p}{\partial \eta}) d\eta + \vec{V}_h \cdot \nabla p \tag{10}$$

c) the vertical velocity in the hybrid coordinate system, needed for the semi-Lagrangian computation of the vertical trajectory:

$$\dot{\eta}\frac{\partial p}{\partial \eta} = -\frac{\partial p}{\partial t} - \int_0^\eta \nabla \cdot (\vec{V}_h \frac{\partial p}{\partial \eta}) d\eta \tag{11}$$

In all equations, the only vertical operator is the vertical integral from the top of the atmosphere (η=0) to the model levels, where all the variables are kept (no vertical staggering), and to the surface (η=1). The integral in the hydrostatic equation (5), which is an integral from the surface to the model levels, can be computed by the difference between the integral from the top of the atmosphere to the model level minus the integral to the surface. Notice that $\frac{\partial p}{\partial \eta}$ is computed with (1), not by vertical differentiation.

4. Vertical integration operator

The finite element methodology is used for constructing an operator that performs the vertical integrals needed, as stated in section 3.

The operation "integral from the top of the atmosphere to a model level"

$$F(\eta) = \int_0^\eta f(x) dx \tag{12}$$

can be approximated as

$$\sum_{i=K_1}^{K_2} C_i d_i(\eta) \approx \sum_{i=M_1}^{M_2} c_i \int_0^\eta e_i(x) dx \tag{13}$$

where C_i are the (unknown) coefficients of the expansion of the unknown function $F(\eta)$ as a linear combination of the basis functions $d_i(\eta)$, a linearly independent set of compact-support functions (finite elements) which form a basis for the domain $0 \le \eta \le 1$.

The quantities c_i are likewise the coefficients of the expansion of the known function $f(\eta)$ as a linear combination of the basis set $\{e_i(\eta)\}$, not necessarily the same set as $\{d_i(\eta)\}$.

We apply now the Galerkin procedure by requesting that the approximation error in equation (13) should be zero in the space spanned by a complete set of test functions $\{t_i(\eta)\}$ (not necessarily the same set as either

the $\{d_i(\eta)\}$ or the $\{e_i(\eta)\}$). Therefore, scalarly multiplying eq. (13) by each of the functions of the set $\{t_i(\eta)\}$ converts the approximate equality into an equality:

$$\sum_{i=K_1}^{K_2} C_i \int_0^1 t_j(x) d_i(x) dx = \sum_{i=M_1}^{M_2} c_i \int_0^1 \left(t_j(x) \int_0^x e_i(y)\, dy \right) dx \qquad \text{for } N_1 \le j \le N_2 \tag{14}$$

In matrix form this set of equations can be written as:

$$\underline{\underline{\mathbf{A}}}\vec{\mathbf{C}} = \underline{\underline{\mathbf{B}}}\vec{\mathbf{c}} \tag{15}$$

where $\vec{C} = (C_{K_1}, C_{K_1+1}, ..., C_{K_2})$, $A_{i,j} = \int_0^1 t_j(x) d_i(x) dx$, $B_{i,j} = \int_0^1 t_j(x) \left(\int_0^x e_i(y) dy \right) dx$ and

$\vec{c} = (c_{M_1}, c_{M_1+1}, ..., c_{M_2})$. From the set of linear equations (15), the coefficients $\vec{\mathbf{C}}$ can be computed provided that matrix $\underline{\underline{\mathbf{A}}}$ is invertible:

$$\vec{\mathbf{C}} = \underline{\underline{\mathbf{A}}}^{-1}\underline{\underline{\mathbf{B}}}\vec{\mathbf{c}} \tag{16}$$

If the function $f(\eta)$ to be integrated is given by its values at the model levels, the set of coefficients c_i has to be computed by projecting $f(\eta)$ on the space of $\{e_i(\eta)\}$. In the case of cubic finite elements, the number of basis functions is the number of model levels plus 4, therefore the projection needs a set of 4 boundary conditions. In the ECMWF model it is assumed that the value of the function is constant and with zero derivative outside the domain spanned by the model levels. Calling $\underline{\underline{\mathbf{S}}}^{-1}$ the projection matrix and $\underline{\underline{\mathbf{P}}}$ the matrix to compute the values of $F(\eta)$ at the model levels plus the surface, given the values of C_i, we can finally write (16) as:

$$\vec{\mathbf{F}} = \underline{\underline{\mathbf{P}}}\, \underline{\underline{\mathbf{A}}}^{-1}\underline{\underline{\mathbf{B}}}\, \underline{\underline{\mathbf{S}}}^{-1}\vec{\mathbf{f}} \equiv \underline{\underline{\mathbf{J}}}\,\vec{\mathbf{f}} \tag{17}$$

where $\vec{\mathbf{f}}$ is the set of values of $f(\eta)$ at the model levels, whereas $\vec{\mathbf{F}}$ is the set of values of $F(\eta)$ at the models levels plus the surface. $\underline{\underline{\mathbf{J}}}$ is called the integration matrix, because applying it to the values of a function to be integrated it returns the values of the integral. From this point of view, the integration scheme can be seen as a finite-difference algorithm, which has been developed using the finite-element formalism.

The accuracy of the algorithm can be shown to be 8th order (Untch and Hortal 2004) when the basis and test functions are chosen to be cubic B-splines. It has also been shown to be 8 times more accurate than solving with the same finite-elements the differential equation problem $f(\eta) = dF(\eta)/d\eta$ (Staniforth and Wood 2004).

In the operational version of the ECMWF forecast model, the sets $\{d_i(\eta)\}$ and $\{t_i(\eta)\}$ are chosen to be the same, which ensures that matrix $\underline{\underline{\mathbf{A}}}$ is symmetric and positive definite. This ensures it is invertible. The set $\{e_i(\eta)\}$ is also identical to $\{d_i(\eta)\}$ except at the boundaries. The basis functions d_0, d_1, and d_2 are linearly combined with d_{-1} so that all of them are zero at η=0. This ensures that $\int_0^0 f(x)dx \equiv 0$ is always fulfilled.

5. The spectral horizontal representation

Most of the scalar forecast fields in the model are represented as a linear combination of spherical harmonics

$$X(\lambda, \mu, \eta, t) = \sum_{m=-N}^{N} \sum_{n=|m|}^{N} X_n^m(\eta, t) Y_n^m(\lambda, \mu) \tag{18}$$

Here $Y_n^m(\lambda,\mu) \equiv P_n^m(\mu)e^{im\lambda}$ are the spherical harmonics, the product of a Fourier function in longitude with zonal wavenumber *m* and an associated Legendre polynomial in $\mu\ (\equiv \sin\phi)$ (where ϕ is the latitude) with total wavenumber *n*. The truncation limit *N* in the second sum corresponds to a triangular truncation, which has the property that it is isotropic, that is, the highest total wavenumber represented is independent of the value of the zonal wavenumber and therefore of the direction of the corresponding wavevector.

The spectral coefficients $X_n^m(\eta,t)$ can be computed taking advantage of the orthogonality properties of the spherical harmonics as:

$$X_n^m(\eta,t) = \frac{1}{4\pi}\int_{-1}^{1}\int_{0}^{2\pi} X(\lambda,\mu,\eta,t)P_n^m(\mu)e^{-im\lambda}d\lambda d\mu \tag{19}$$

The integral with respect to longitude (direct Fourier transform) can be computed exactly by means of the Fast Fourier Transform (FFT) algorithm if points equally spaced in longitude are used in a number of at least 2N+1 (as in the so called linear grid). The aliasing produced in physical space when two functions are multiplied together can be eliminated if we use a number of points in the FFT of at least 3N+1 (quadratic grid). Likewise the integral in latitude (direct Legendre transform) can be computed exactly by means of a Gaussian quadrature formula using a number of latitudes of at least (2N+1)/2 (case of the linear grid) and the quadratic aliasing eliminated if at least (3N+1)/2 latitudes are used.

A very important property of the spherical harmonics is that they are eigenfunctions of the Laplacian operator:

$$\nabla^2 Y_n^m = -\frac{n(n+1)}{a^2}Y_n^m \tag{20}$$

This property makes solving a Helmholtz equation trivial in spectral space. Also the horizontal derivatives of a field can be computed analytically in spectral space.

The quantities represented in spectral space related with the momentum equation are vorticity and divergence, which are true scalars, unlike the wind components, and can therefore be represented in terms of spherical harmonics.

One possible drawback of the spectral method is that the Legendre transforms take a number of operations proportional to N^3. The cost of the rest of the computations is only proportional to N^2. When the resolution is increased, eventually the Legendre transforms will become the main cost of the integration of the equations. For more details on this subject see the contribution of Clive Temperton in this seminar proceedings.

The distribution of points in physical space described above, which allows exact Fourier and Legendre transforms, is called the full Gaussian grid. In this grid, the geographical longitudinal distance between grid points is very small near the pole, compared with the corresponding distance near the equator, due to the smaller length of a latitude circle. The latitudinal distance is about the same near the poles and near the equator. The resolution is therefore very anisotropic, which is not consistent with the isotropy of the triangular spectral representation. In order to make the two representations more consistent, the number of points per row of latitude can be made smaller as we approach the poles. The resulting distribution of points is called the reduced Gaussian grid and the total number of points is of the order of 33% smaller that in the full Gaussian grid, making the computations in grid-point space ~33% cheaper. More details can be found in Hortal and Simmons (1991) and in Courtier and Naughton (1994).

6. Semi-implicit time integration scheme

A time discretization in which the right-hand-side (r.h.s.) of the equation is taken at the centre of the time interval is an explicit second-order discretization. It is normally subject to a CFL-like stability limit. If the r.h.s. of the equation is taken as the average between its value at the initial time and its value at the final time, the discretization is called implicit and gives generally a stable scheme. An alternative is to treat implicitly only a linearized form of the r.h.s.. This is called semi-implicit scheme and can lead to a simpler equation to solve. The conversion of an explicit scheme into an implicit or semi-implicit one can be achieved by adding an "implicit correction term"

$$\Delta_{tt} X \equiv 0.5\left(X^{+} + X^{-}\right) - X^{0} \tag{21}$$

where X is the part of the r.h.s. we want to treat implicitly, superscript 0 indicates the value used in the explicit discretization, superscript - and + indicate the values at the initial and final moments of the time step.

With this notation, the semi-implicit method used at ECMWF can be written as:

$$\frac{d\vec{V}}{dt} = RHS_V + \Delta_{tt}\left\{\underset{\approx}{\gamma}\nabla_h T + R_d T_r \nabla_h\left(\ln p_s\right)\right\} \tag{22}$$

$$\frac{dT}{dt} = RHS_T + \Delta_{tt}\left(\underset{\approx}{\tau} D\right) \tag{23}$$

$$\frac{d}{dt}(\ln p_s) = RHS_p + \Delta_{tt}\left(\underset{\sim}{\nu} D\right) \tag{24}$$

where the operator Δ_{tt} is applied in (22) to the pressure-gradient term linearized around a reference temperature T_r and a reference surface pressure ($p_{s)r}$, in (23) to the linearized energy conversion term and (24) to the linearized r.h.s. of (9). The operators $\underset{\approx}{\gamma}$, $\underset{\approx}{\tau}$ and $\underset{\sim}{\nu}$ are defined by:

$$(\underset{\approx}{\gamma} X)_\eta = -\int_1^\eta R_d X \frac{d}{d\eta'}\left(\ln p_r\right) d\eta' \tag{25}$$

$$(\underset{\approx}{\tau} X)_\eta = \kappa T_r \left(\frac{1}{p_r}\right)_\eta \int_0^\eta X \frac{dp_r}{d\eta'} d\eta' \tag{26}$$

and

$$\underset{\sim}{\nu} X = \frac{1}{(p_s)_r}\int_0^1 X \frac{dp_r}{d\eta} d\eta\,. \tag{27}$$

Here p_r is the pressure computed with (1) using as surface pressure the reference surface pressure $(p_s)_r$. The vertical integrals are performed with the operator defined in Section 4.

Discretizing in time equations (22), (23) and (24) and eliminating the temperature and the surface pressure at the future time step, we arrive at a set of coupled Helmholtz equations for the value of the divergence at the future time step:

$$\left(\underset{\approx}{\mathbf{I}} + \underset{\approx}{\mathbf{\Gamma}}\nabla_h^2\right) D^{+} = \tilde{D} \tag{28}$$

where $\underset{\approx}{\mathbf{\Gamma}} \equiv \underset{\approx}{\gamma}\underset{\approx}{\tau} + R_d T_r \underset{\sim}{\nu}$ couples the equations in the vertical. The set (28) is decoupled by projecting onto the space of eigenvectors of matrix $\underset{\approx}{\mathbf{\Gamma}}$. This leads to a Helmholtz equation for every eigenvalue of $\underset{\approx}{\mathbf{\Gamma}}$. These Helmholtz equations are trivial to solve in spectral space.

7. Semi-Lagrangian advection

For the benefit of the readers who are not familiar with the semi-Lagrangian procedure, we outline here briefly the basic ideas.

In the Lagrangian point of view, time is the only independent variable. The entities considered are individual air parcels and the space coordinate should be consistent with time, according to the movement of the corresponding air parcel. According to this point of view, the advection equation without r.h.s.

$$\frac{d\varphi}{dt} = 0 \tag{29}$$

can be interpreted as follows: "the property φ of an air parcel does not change with time", i.e. it is conserved. A two-time-level discretization of this equation is:

$$\frac{\varphi(x_j, t+\Delta t) - \varphi(x_*, t)}{\Delta t} = 0 \tag{30}$$

where x_j is the position at time $t+\Delta t$ of the parcel of air considered and x_* its position at time *t*. The problem with the Lagrangian point of view is that a set of parcels evenly distributed in space (for example at the points of a Gaussian grid) end up unevenly distributed at the end of the time step and therefore operations such as the spectral transforms can no longer be performed on them.

The semi-Lagrangian procedure solves this difficulty by considering the set of air parcels which will arrive at the set of evenly distributed grid points at the future time and traces back their positions at the present time (or the previous time in a three-time-level scheme). As these positions will in general not be grid points, the value of the property φ has to be found by interpolation from its value at the surrounding grid points, where the values are known.

According to the linear stability analysis, in the case of constant advection velocity U_0, this semi-Lagrangian procedure is absolutely stable. In this case, finding the departure point of a parcel of air can be done by discretizing in the semi-Lagrangian way the definition of the velocity of that air parcel:

$$\frac{dx}{dt} = U_0 \Rightarrow \frac{x_j - x_*}{\Delta t} = U_0 \Rightarrow x_* = x_j - U_0 \Delta t\,. \tag{31}$$

When the advection equation has a right hand side

$$\frac{d\varphi}{dt} = R \tag{32}$$

a centred (second-order accurate) three-time-level discretization can be given by:

$$\frac{\varphi^A(t+\Delta t) - \varphi^D(t-\Delta t)}{2\Delta t} = R^M(t) \tag{33}$$

where we have introduced the following notation: superscript A means evaluated at the arrival point, superscript D means evaluated at the departure point and superscript M means evaluated at the centre of the trajectory.

Three-time-level schemes have two main disadvantages:

- they are less efficient than two-time-level schemes
- they produce a computational mode.

A two-time-level scheme similar to (33) is

$$\frac{\varphi^A(t+\Delta t)-\varphi^D(t)}{\Delta t}=R^M(t+\frac{\Delta t}{2}) \tag{34}$$

where the value of the r.h.s. has to be evaluated at an instant in time half way between the present and the future time steps. A possibility is to extrapolate the r.h.s. R in time:

$$R(t+\frac{\Delta t}{2})\approx\frac{3}{2}R(t)-\frac{1}{2}R(t-\Delta t) \tag{35}$$

but the corresponding scheme happens to be unstable. A consequence of this instability can be seen in Figure 1, where the forecast map of temperature at 200 hPa appears very noisy.

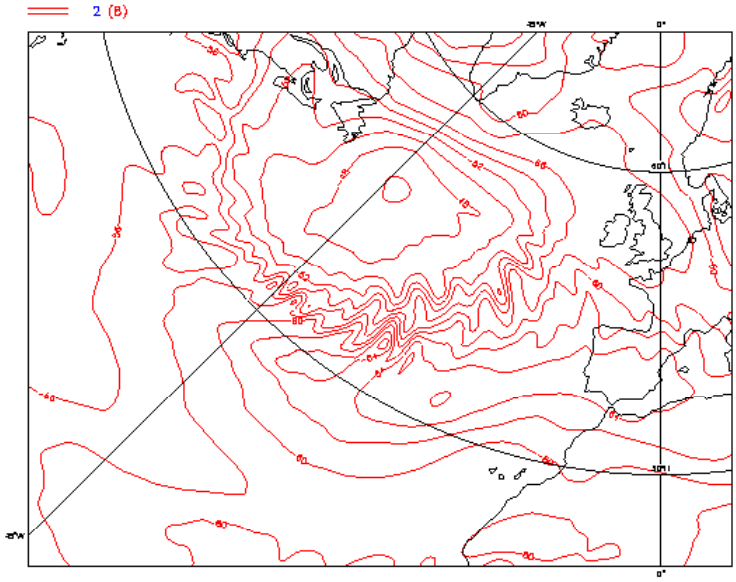

Figure 1 Forecast of 200 hPa temperature from 4 Jan 1997

An alternative second-order accurate scheme has been developed, starting from a Taylor series expansion of the function φ around the present time step (and therefore the departure point of the semi-Lagrangian trajectory of the corresponding air parcel):

$$\varphi^A(t+\Delta t)\approx\varphi^D(t)+\Delta t\cdot\left(\frac{d\varphi}{dt}\right)_t^D+\frac{(\Delta t)^2}{2}\cdot\left(\frac{d^2\varphi}{dt^2}\right)_{AV} \tag{36}$$

and then substituting, according to the advection equation,

$$\left(\frac{d\varphi}{dt}\right)_t^D=R^D(t) \tag{37}$$

and

$$\left(\frac{d^2\varphi}{dt^2}\right)_{AV}=\left(\frac{dR}{dt}\right)_{AV}\approx\frac{R^A(t)-R^D(t-\Delta t)}{\Delta t}. \tag{38}$$

The approximation in (38) is the closure of the scheme and it implies a small inconsistency with the pure Lagrangian point of view, because the value of R at the present time step is taken at the arrival point of the trajectory and the value at the departure point is taken from the previous time step. It is therefore a kind of extrapolation in time, but a linear stability analysis shows that its stability is almost independent of the size

of the time-step (see Hortal 2002). For this reason it has been named Stable Extrapolation Two-Time-Level Semi-Lagrangian scheme (SETTLS).

With this scheme, the forecast shown in Figure 1 was recomputed and the result is shown in Figure 2.

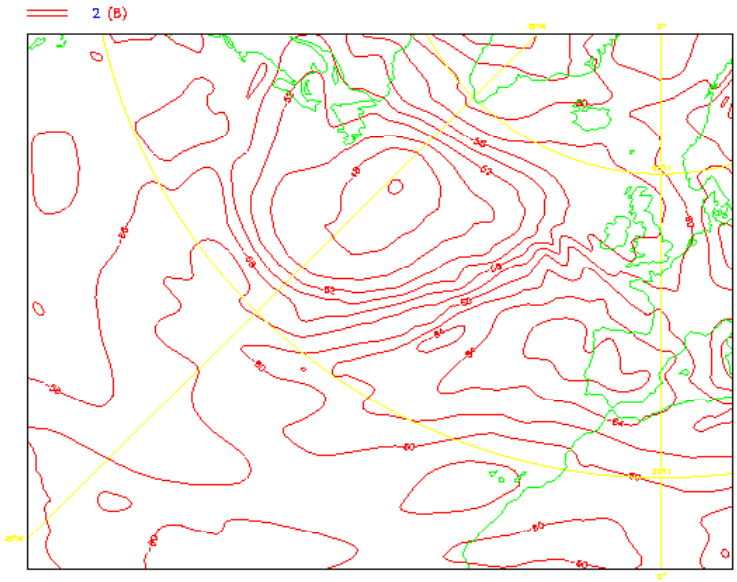

Figure 2 As Figure 1 but using the SETTLS scheme

There are some problems that require care when coding semi-Lagrangian advection in spherical geometry. As stated earlier, the momentum equation is discretized in vector form because a vector is continuous across the poles, while their components are not. When performing the interpolations to the departure points of the semi-Lagrangian trajectories we nevertheless interpolate u and v, which are the components of the vector wind relative to the system of reference local at the departure point. The interpolated value has to be used at the arrival point as the value of the wind at the future time. As the system of reference at that point is different to the one at the departure point, the corresponding change of reference system has to be performed.

Another problem is the following: if we consider the vector wind constant during one time step in the computation of the semi-Lagrangian trajectories and this wind is horizontal at the departure point, it will no longer be horizontal at the arrival point, due to the curvature of the sphere. Therefore, the equivalent assumption of constant horizontal velocity in plane geometry should be constant angular velocity over the surface of the sphere, the trajectory being the arc of a great circle instead of a straight line.

Interpolations used in the semi-Lagrangian scheme

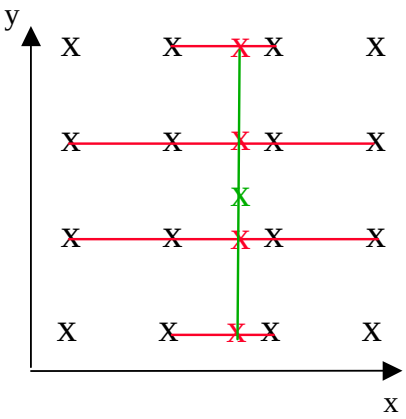

Suppose we have a departure point at the green X positioning in the diagram to the left. In two dimensions, a bi-cubic interpolation will involve 4 cubic interpolations in the x-direction direction followed by one cubic interpolation in the y direction. In three dimensions the number of cubic one-dimensional interpolations will be 21. In order to save on the amount of computations, the only cubic interpolations performed in the ECMWF forecast model are the ones closest to

the departure point, the rest being substituted by linear interpolations, as in the first and fourth rows of the above diagram. At the second level above the departure point and the second level below the departure point the two-dimensional interpolation is therefore bilinear. In three dimensions the total number of interpolations is: 7 cubic and 10 linear. The computational cost is therefore a lot reduced. The forecast accuracy is however not reduced significantly by the substitution of these cubic interpolations by linear interpolations. This procedure is called quasi-cubic interpolation.

Suppose we have a departure point at the green X positioning in the diagram to the left. In two dimensions, a bi-cubic interpolation will involve 4 cubic interpolations in the x-direction direction followed by one cubic interpolation in the y direction. In three dimensions the number of cubic one-dimensional interpolations will be 21. In order to save on the amount of computations, the only cubic interpolations performed in the ECMWF forecast model are the ones closest to the departure point, the rest being substituted by linear interpolations, as in the first and fourth rows of the above diagram. At the second level above the departure point and the second level below the departure point the two-dimensional interpolation is therefore bilinear. In three dimensions the total number of interpolations is: 7 cubic and 10 linear. The computational cost is therefore a lot reduced. The forecast accuracy is however not reduced significantly by the substitution of these cubic interpolations by linear interpolations. This procedure is called quasi-cubic interpolation.

The cubic interpolations are done by means of cubic Lagrange polynomials. In one dimension a cubic polynomial is defined which fits the four neighbouring points to the departure point (the four points on a red line in the diagram). The interpolated value is then the value of the polynomial at the position of the departure point.

When the function to be interpolated is rough, a cubic interpolation can produce an interpolated value larger or smaller than all the values used for the interpolation. In an advection process, however, no new maxima or minima of the advected function should be produced. The cubic interpolation can therefore produce artificial maxima or minima of the function being advected, which are not physical, and which can lead to a production of excessive eddy kinetic energy during a forecast. In order to avoid this problem, the following procedure is used: if the interpolated value in any of the one-dimensional cubic interpolations is larger/smaller than both of the surrounding values (the two inner points used in the interpolation), the interpolated value is set to the corresponding border value of the interval defined by these two values (i. e. if the interpolated value is larger than the values of the function at both nearest neighbouring points, the interpolated value is taken to be the larger of the two values, and if it is smaller than both values, then it is taken to be the smaller of the two). This procedure is called quasi-monotone interpolation (Bermejo and Staniforth 1992) and is applied in the horizontal to all variables and in the vertical to humidity and ozone only.

Another problem of the cubic interpolation is that the accuracy of the interpolation, compared with a spectral representation of the function, is much reduced when the interpolated function is rough. In order to reduce this problem in the model, the surface pressure tendency equation and the thermodynamic equation are modified such that the quantities to be advected (i.e. interpolated) are smoother than the original quantities ln p_s and T respectively (see Ritchie and Tanguay 1996 for the surface pressure equation and Temperton et al. 2001 for the thermodynamic equation). In an isothermal atmosphere with temperature $\overline{T}$, the logarithm of the surface pressure changes with the height of the orography Φ_s according to:

$$l^* = \frac{\Phi_s}{R_d \overline{T}} \tag{39}$$

The variable ln p_s in eq. (9) is written as the sum of l^* and a remainder l'. The part involving l^* is moved to the r.h.s. of the equation and treated together with the rest of the terms there. The total time derivative is split

into partial time derivative and horizontal and vertical advection, of which only the horizontal advection part is different from zero as l^* is independent of time and of the vertical coordinate. Only the remainder l', which is much smoother than ln p_s, is treated in the semi-Lagrangian way and needs to be cubically interpolated to the departure points of the trajectories.

$$\frac{dl'}{dt} = [RHS] + \frac{1}{R_d \overline{T}} \vec{V}_h \cdot \nabla \phi_s \tag{40}$$

The result is a much improved mass conservation in the model: a 10-day forecast run at T106 resolution using cycle 13R4 of the operational model lost 0.59 hPa in the global mean p_s, compared with the analysis value, using the original formulation of the pressure tendency equation, and only 0.02 hPa if the modified formulation was used.

In the thermodynamic equation a similar "trick" is applied. The advected variable is not T itself but (T-T_b) where

$$T_b = -\left(p_s \frac{\partial p}{\partial p_s} \frac{\partial T}{\partial p} \right)_{ref} \cdot \frac{\phi_s}{R_d \overline{T}} \tag{41}$$

is an approximation to the change of temperature with height in the standard atmosphere. The modified thermodynamic equation is then

$$\frac{d(T - T_b)}{dt} = [RHS]_T - (\vec{V}_h \cdot \nabla T_b) - \dot{\eta} \frac{\partial T_b}{\partial \eta} \tag{42}$$

because T_b is independent of time but not of the vertical dimension.

T-T_b is a much smoother function over orography than T and the result of using the new formulation is a reduced level of noise in all fields, mostly vertical velocity, over orography.

When searching for the departure points of the semi-Lagrangian trajectories, as the wind is not constant as in eq. (31), the velocity in the equation $d\vec{R}/dt = \vec{V}$ (where $\vec{R}$ is the position vector of the air parcel) has to be treated according with the SETTLS scheme and therefore $\vec{V}$ at the present time needs to be interpolated to the departure point. However, the departure point is not known, it is what we are searching for, and therefore the procedure has to be iterative. For interpolating the r.h.s. of the equations at the departure point, both for the velocity equation and for the forecast equations, only linear interpolations in the three dimensions are used. Tests show no significant degradation in the forecast accuracy compared with using cubic interpolations, which are much more expensive. In some forecasts, in the stratospheric polar night jet, when it is displaced from the pole, a feedback process takes place between the computation of the vertical part of the semi-Lagrangian trajectories and the solution of the evolution equations. This feedback leads to a resonance of certain wavelengths that can produce a very noisy forecast of the divergence as the one shown in Figure 3a.

In order to reduce this feedback, a smoothing interpolation is applied to the vertical velocity in the stratosphere in the computation of the vertical part of the semi-Lagrangian trajectories. This smoothing interpolation uses the same points as a cubic Lagrange interpolation, but instead of fitting a cubic polynomial, a linear function is fitted by means of least square distance to the points. The corresponding "interpolated" value is a filtered version of the vertical velocity, even when the interpolation point coincides with a grid point (the procedure is also applied at the arrival point of the trajectories, which are the grid points). The resulting forecast divergence using this smoothing interpolation for interpolating the vertical velocity is shown in Figure 3b. The resonance process that leads to the amplification of specific waves has been suppressed while the "real" waves are only marginally affected.

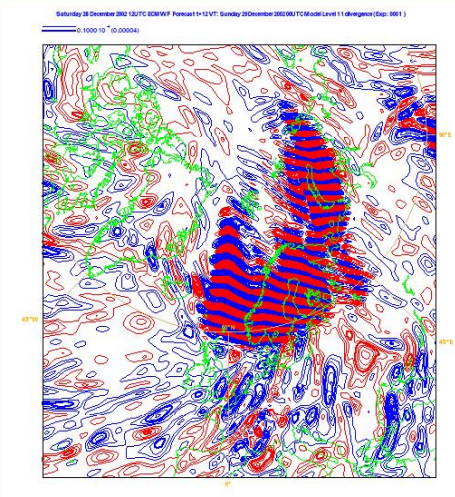

Figure 3a

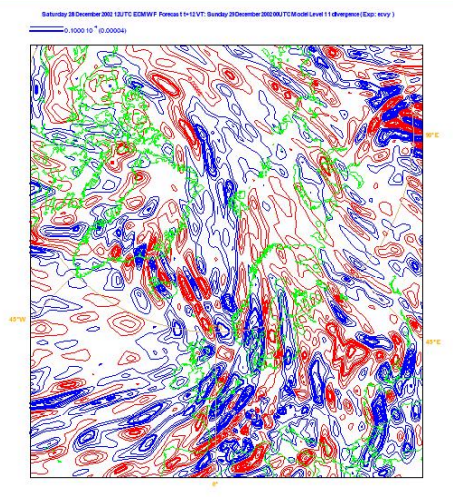

Figure 3b

8. Treatment of the Coriolis term

The Coriolis term $f\vec{k}\times\vec{V}_h$ in eq. (3) can be treated explicitly with the rest of the r.h.s. of the equation in a three-time-level scheme. In a two-time-level scheme, on the other hand, extrapolation in time of this term leads to instability (Temperton 1997).

Two possibilities exist in the ECMWF forecast model for treating the Coriolis term in the two-time-level semi-Lagrangian scheme: the advective treatment and the implicit treatment.

In the advective treatment, the Coriolis term is written as

$$f\vec{k}\times\vec{V}_h = 2\vec{\Omega}\times\frac{d\vec{R}}{dt}$$

therefore the left hand side of the momentum equation is modified as follows:

$$\frac{d\vec{V}_h}{dt} + f\vec{k}\times\vec{V}_h \rightarrow \frac{d}{dt}(\vec{V}_h + 2\vec{\Omega}\times\vec{R}) \tag{43}$$

and the quantity advected with the semi-Lagrangian procedure is $\vec{V}_h + 2\vec{\Omega}\times\vec{R}$ instead of only the horizontal wind.

In the implicit treatment the value of the Coriolis term is taken as the average between the value at the present time step and the value at the future time step.

$$\frac{\vec{V}_h^{+} - \vec{V}_h^{0}}{\Delta t} = -f\vec{k}\times 0.5(\vec{V}_h^{+} + \vec{V}_h^{0}) + \ldots \tag{44}$$

This causes the Helmholtz equations for the individual spectral components of divergence to become partially coupled and leads therefore to the need of solving a tri-diagonal problem instead of a diagonal problem in spectral space.

9. Physical parameterizations

The treatment of the terms P_x in eq. (3), (4), (7) and (8) are coupled with the semi-Lagrangian scheme. Details are given in the presentation by Anton Beljaars in this proceedings.

10. Horizontal diffusion

The terms K_x in the forecast equations are the contributions from horizontal diffusion. At ECMWF we use harmonic 4th order diffusion:

$$\frac{\partial X}{\partial t} = -K\nabla^4 X \tag{45}$$

The solution of this equation is very easy in spectral space and therefore the application of the horizontal diffusion is done in a time-split way from the rest of the terms in the equations and applied in spectral space after the solution of the Helmholtz equation produced by the semi-implicit time scheme. Two possibilities exist in the ECMWF forecast model for the horizontal diffusion:

Implicit (backward) formulation

$$\frac{X_{n,m}(t+\Delta t) - X_{n,m}(t)}{\Delta t} = -K\nabla^4 X_{n,m}(t+\Delta t) = -K\left(\frac{n(n+1)}{a^2}\right)^2 X_{n,m}(t+\Delta t)$$

$$\Rightarrow X_{n,m}(t+\Delta t) = X_{n,m}(t)\frac{1}{1+K\Delta t\left(\frac{n(n+1)}{a^2}\right)^2}$$

Analytical solution

$$\frac{\partial X_{n,m}}{\partial t} = -K\left(\frac{n(n+1)}{a^2}\right)^2 X_{n,m} \Rightarrow X_{n,m}(t+\Delta t) = X_{n,m}(t)e^{-K\Delta t\left(\frac{n(n+1)}{a^2}\right)^2}$$

11. Summary of the main numerical features in the ECMWF atmospheric forecast model

- Two-time-level semi-Lagrangian advection
  - SETTLS scheme
  - Quasi-monotone quasi-cubic interpolation
  - Linear and smoothing interpolations for the r.h.s. of the equations
  - Modified continuity and thermodynamic equations
- Semi-implicit treatment of linearized adjustment terms
- Cubic finite-elements for the vertical integrals
- Spectral horizontal Helmholtz solver (and computation of horizontal derivatives)
- Linear reduced Gaussian grid
- Semi-Lagrangian coupling of physics and dynamics

12. Future developments

- Test/develop a non-hydrostatic version of the forecast model.
- Improve the semi-Lagrangian interpolations.
- Try a horizontal representation by means of double Fourier series instead of spherical harmonics (this will avoid the Legendre transforms).

- Improve the conservation of advected quantities.
- Study the influence of the upper and lower boundary conditions
    - for the semi-Lagrangian advection
    - for the vertical finite-element representation.
- Investigate noise on vorticity over orography (aliasing?).

13. References

Bermejo, R. and Staniforth, A. (1992): The conversion of semi-Lagrangian advection schemes to quasi-monotone schemes. *Mon. Weather Rev.,* **120**, pp. 2622-2632

Courtier, P. and Naughton, M. (1994): A pole problem in the reduced Gaussian grid. *Q.J.R. Meteorol. Soc.*, **120**, pp. 1389-1407

Hortal, M. and Simmons, A.J. (1991): Use of reduced Gaussian grids in spectral models. *Mon. Wea. Rev.*, **119**, pp. 1057-1074

Hortal, M. (2002): The development and testing of a new two-time-level semi-Lagrangian scheme (SETTLS) in the ECMWF forecast model. *Q.J.R. Meteorol. Soc* **128**, pp. 1671-1687

Ritchie, H. and Tanguay, M. (1996): A comparison of spatially averaged Eulerian and semi-Lagrangian treatments of mountains. *Mon. Weather Rev.* **124**, pp. 167-181

Ritchie, H. Temperton, C. Simmons, A. Hortal, M. Davies, T. Dent, D. and Hamrud, M. (1995): Implementation of the semi-Lagrangian method in a high-resolution version of the ECMWF forecast model. *Mon. Wea. Rev.* **123,** pp,489-514

Simmons, A.J. and Burridge, D.M. (1981): An energy and angular-momentum conserving vertical finite-difference scheme and hybrid vertical coordinates. *Mon. Wea. Rev.* **109,** pp.758-766

Staniforth, A. and Wood, N. (2004): Comments on the paper "A finite-element scheme for the vertical discretization of the semi-Lagrangian version of the ECMWF forecast model" by A Untch and M Hortal. *Submitted to Q.J.R. Meteorol. Soc*

Temperton, C. (1997): Treatment of the Coriolis terms in semi-Lagrangian spectral models. *The André J. Robert memorial volume,* Canadian Meteorological and Oceanographical Society, pp. 293-302, Ottawa, Canada

Temperton, C. Hortal, M. and Simmons, A.J. (2001): A two-time-level semi-Lagrangian global spectral model. *Q.J.R. Meteorol. Soc.* **127**, pp. 111-127

Untch, A. and Hortal, M. (2004): A finite-element scheme for the vertical discretization of the semi-Lagrangian version of the ECMWF forecast model. *Q.J.R. Meteorol. Soc.* **130**, pp. 1505-1530